

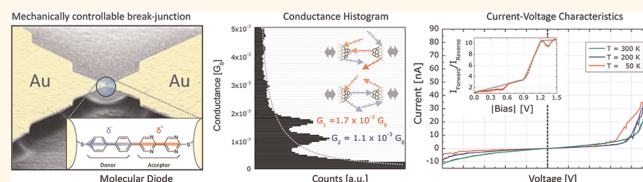
# Transport Properties of a Single-Molecule Diode

Emanuel Lörtscher,<sup>†,\*</sup> Bernd Gotsmann,<sup>†</sup> Youngu Lee,<sup>‡</sup> Luping Yu,<sup>§</sup> Charles Rettner,<sup>⊥</sup> and Heike Riel<sup>†</sup>

<sup>†</sup>IBM Research-Zurich, Säumerstrasse 4, 8803 Rüschlikon, Switzerland, <sup>‡</sup>Energy Systems Engineering, Daegu Gyeongbuk Institute of Science and Technology, 50-1, Sang-ri, Hyeonpung-myeon, Dalseong-gun, Daegu, Korea, <sup>§</sup>Department of Chemistry and The Frank Institute, The University of Chicago, 929 East 57th Street, Chicago, Illinois 60637, United States, and <sup>⊥</sup>IBM Research-Almaden, San Jose, California, 95120, United States

Molecular electronics is aimed at the use of small ensembles or even single molecules as functional building blocks in electronic circuits.<sup>1,2</sup> Besides current-switching and charge-storing functionalities embodied in a molecule, current rectification is one of the most basic requirements for any electronic application. Single-molecule diodes are of crucial importance because they enable, for example, the electrical addressing of an individual molecular node in an ultimately scaled cross-bar-type architecture, where the node consists of an ensemble or only of a single functional molecule with both current-rectifying and switching/storing moieties. In 1974, the visionary concept introduced by Aviram and Ratner<sup>1</sup> for a single-molecule diode composed of a donor moiety electronically decoupled *via* a nonconjugated  $\sigma$ -bridge from an acceptor moiety was still far away from realization both chemically and experimentally. Nevertheless, several rectification mechanisms in single molecules have been discussed in the past. The Aviram–Ratner approach considers a donor–insulator–acceptor configuration.<sup>1</sup> The donor and acceptor units are placed on the same molecule close to the left or right electrode, respectively. The two electrodes are connected through three tunneling barriers, linking one electrode to the donor unit, the donor unit to the acceptor unit, and the acceptor unit to the other electrode, respectively. In the Aviram–Ratner proposal, at zero applied voltage bias, the LUMO of the acceptor is slightly above the electrode's Fermi energy and the HOMO of the acceptor is slightly below. Upon application of a voltage bias across the junction, the LUMO (or the HOMO) can be aligned to the Fermi energy of the leads, or separated depending on the bias direction. Ellenbogen and Love considered a similar system where a single LUMO was used for both

## ABSTRACT



Charge transport through single diblock dipyrimidinyl diphenyl molecules consisting of a donor and acceptor moiety was measured in the low-bias regime and as a function of bias at different temperatures using the mechanically controllable break-junction technique. Conductance histograms acquired at 10 mV reveal two distinct peaks, separated by a factor of 1.5, representing the two orientations of the single molecule with respect to the applied bias. The current–voltage characteristics exhibit a temperature-independent rectification of up to a factor of 10 in the temperature range between 300 and 50 K with single-molecule currents of 45–70 nA at  $\pm 1.5$  V. The current–voltage characteristics are discussed using a semiempirical model assuming a variable coupling of the molecular energy levels as well as a nonsymmetric voltage drop across the molecular junction, thus shifting the energy levels accordingly. The excellent agreement of the data with the proposed model suggests that the rectification originates from an asymmetric Coulomb blockade in combination with an electric-field-induced level shifting.

**KEYWORDS:** molecular electronics · mechanically controllable break-junction · rectification · single-molecule transport

donor and acceptor moieties.<sup>3</sup> The mechanism underlying the Aviram–Ratner proposal uses the electric field between the electrodes to shift the energy levels of the molecular orbitals according to their energetic position in the gap. Later, this mechanism has been generalized to a simpler system with only one molecular orbital attached to the electrodes through tunneling barriers.<sup>4</sup> In this approach, the position of the orbital is not symmetric in the center between the electrodes but is closer to one of them. This orbital, say a LUMO slightly above the Fermi energy at zero bias, is then aligned or misaligned with the Fermi energy of the electrodes depending on the bias

\* Address correspondence to eml@zurich.ibm.com.

Received for review January 30, 2012 and accepted May 14, 2012.

Published online May 14, 2012  
10.1021/nn300438h

© 2012 American Chemical Society

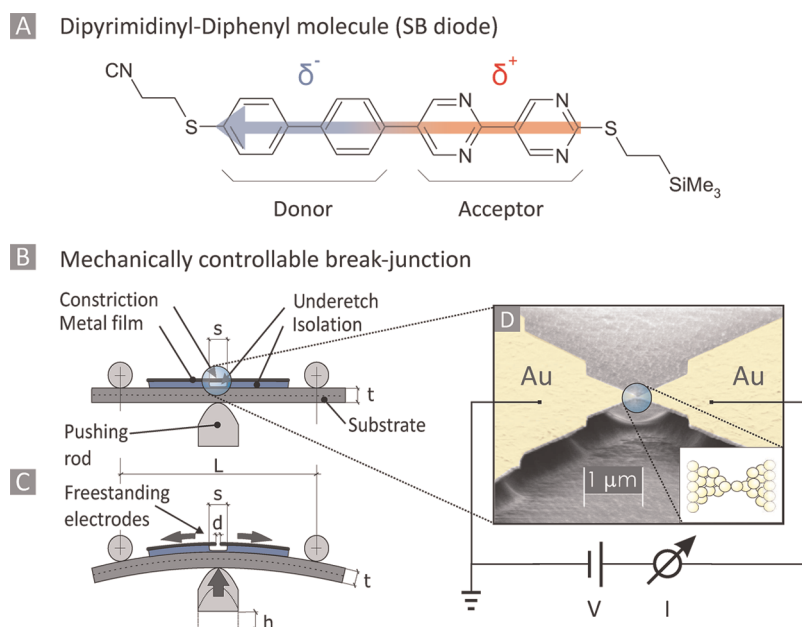


**Figure 1.** (A) Molecular structure of the dipyrimidinyl diphenyl diode (SB) molecule with donor and acceptor moieties. The asymmetric cyanoethyl and trimethylsilylethyl thiol-protecting groups are attached for directed growth. (B) Three-point bending mechanism in which a microfabricated bridge (D) is structured on top of a flexible substrate which can be bent (C) to elongate and finally break the Au bridge. By releasing the pushing rod, the junction can be closed again with subatomic resolution.

direction. The asymmetric positioning of the molecular orbitals in the junction can be controlled by the design of the molecule.<sup>4</sup> However, the required asymmetry may also occur for uncontrolled asymmetric binding of a symmetric molecule to the electrodes<sup>5</sup> and can be considered the reason for generally asymmetric current–voltage,  $I$ – $V$ , curves in many published data.

Both of these pictures, the Aviram–Ratner and the asymmetric coupling, predict rectification in single-molecular diodes through arguments of electric field alone. However, typically single-molecular devices with tunneling barriers to the electrodes show strong charging effects. Consider a molecule placed in such a way that the conducting orbital shifts symmetrically with respect to the applied bias. In addition, let us assume that the tunneling rates are different between the orbital and the two electrodes. In the resonant tunneling condition, this implies that the average population of the orbital with electrons depends on the bias direction.<sup>6</sup> Again, this leads to rectification behavior. Although this mechanism cannot be easily separated from asymmetric coupling to the electric field as described above, it can be considered as a distinct mechanism of rectification, too. In principle, molecules can be designed that allow for better coupling to either of the electrodes while keeping the resonant orbital positioned in the center.

As for experimental verifications, it is not easy to distinguish between the three discussed mechanisms (Aviram–Ratner, asymmetric field, asymmetric charging) for several reasons: The pure Aviram–Ratner diode is very difficult to chemically synthesize. A complete decoupling of the donor and acceptor

orbitals is not always guaranteed. Furthermore, experimental transport measurements suffer from uncontrolled coupling to the metal electrodes due to dependence of the coupling on the exact atomic configuration of the anchoring group with the metal electrodes.

Despite these challenges, several impressive demonstrations of molecular and single-molecule rectification have been published. For example, fabricating self-assembled monolayers (SAMs), as well as in manipulating and controlling single molecules and atoms, enabled several experiments which showed molecular rectification. In 1997, Metzger *et al.* demonstrated that a Langmuir–Blodgett monolayer of zwitterionic hexadecylquinolinium tricyanoquinodimethanide molecules sandwiched between two Au electrodes shows unimolecular rectification behavior with a rectification ratio of up to  $\approx 13$ .<sup>7,8</sup> Also rectification on a single-molecule level has been demonstrated on a SAM system by Ng *et al.*,<sup>9</sup> with a rectification ratio of  $\approx 7$ . Jiang *et al.*<sup>10</sup> used STM techniques on SAMs and obtained a rectification of  $\approx 7$ . Elbing *et al.*<sup>11</sup> observed single-molecule rectification of  $\approx 5$ . The same molecule as used in the present study exhibited rectification of  $\approx 2.5$  in a SAM.<sup>12</sup> The differences among the various experimental approaches are well-described in a recent review on the field of molecular electronics.<sup>13</sup>

## RESULTS AND DISCUSSION

**Acceptor–Donor Diblock Molecule.** In this work, a single-molecular compound with acceptor and donor moieties but without an insulating  $\sigma$ -bridge was studied in terms of its rectification behavior on a single-molecule

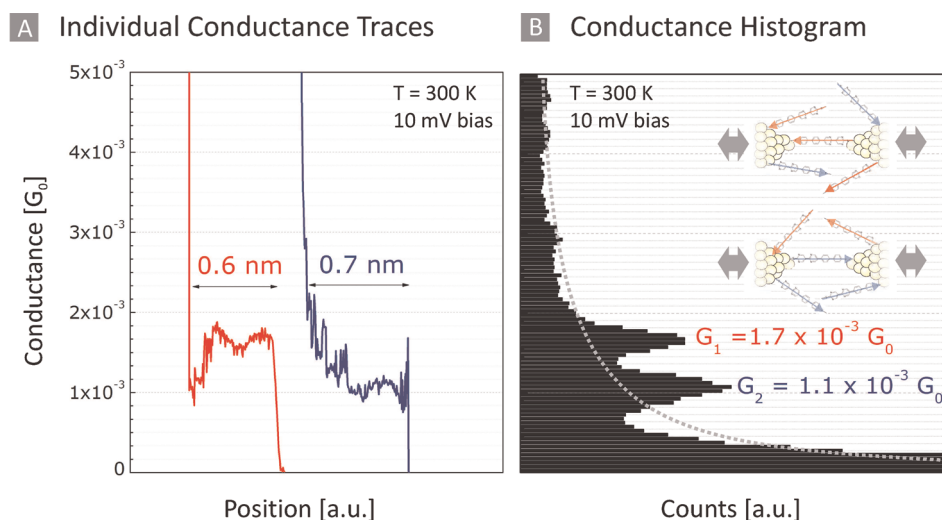


**Figure 2.** (A) Individual conductance traces for Au–diode–Au junction with typical lengths of 0.7 nm measured upon breaking. The short trace lengths and their narrow distribution (see Supporting Information) indicate that the same number of molecules is measured in the repeated cycles, and that the two accumulations in (B) are originating from the two different polarizations rather than from different numbers of molecules being probed. (B) Histograms of 500 opening cycles (taken at 10 mV and 300 K) exhibit two distinct peaks at approximately  $1.1 \times 10^{-3} G_0$  and  $1.7 \times 10^{-3} G_0$ . The gray dotted line shows an exponential fit of the electron tunneling background acquired prior to the application of molecules using the same sample. The appearance of two conductance peaks indicates that, on an average, the molecules bridging the gap have two different conductances depending on how they are situated in the junction with respect to the applied bias and their dipole moments. The data represent raw data as mentioned in the text.

level. The synthesis<sup>14</sup> of the diblock dipyrimidinyl diphenyl (SB) molecule yields an electron-deficient bipyrimidinyl moiety (acceptor) and an electron-rich biphenyl moiety (donor), hence creating a molecular backbone structurally similar to the Aviram–Ratner proposal regarding acceptor–donor blocks. However, the broken intramolecular coupling between the moieties as given by the  $\sigma$ -bond in the seminal Aviram–Ratner proposal<sup>1</sup> is not present. In our work, the donor and the acceptor moieties are covalently linked (Figure 1A), and an electronic overlap between the two subsystems is present. Due to the tilt angle between the donor and acceptor moiety, the maximum conjugation is reduced. The asymmetric electron density of the molecular backbone due to the acceptor–donor configuration causes a permanent dipole moment along the molecular axis. Owing to the different thiol-protecting end groups, the molecule can be self-assembled sequentially and hence be prepared in a directed manner with a specific orientation with respect to the substrate.<sup>12,14</sup> First, the cyanoethyl-protecting group is released by sodium ethoxide (NaOEt), and then, after covalent attachment to the substrate surface, the trimethylsilylethyl-protecting group can be removed by tetrabutylammonium fluoride (TBAF) in THF. This directed-growth approach cannot be employed in our single-molecule experiments using the mechanically controllable break-junction (MCBJ),<sup>15,16</sup> as both electrodes cannot be selectively exposed to the solution of molecules. Here, we deprotect both anchor groups simultaneously, and hence, the orientation of the molecule in the junction cannot be

controlled. However, using our statistical measurement approach,<sup>17</sup> we can investigate the transport properties of the single-molecule junction during repeated formation and breaking cycles (see Experimental Section), thus probing different junction geometries.

**Low-Bias Conductance Histograms.** We studied the low-bias conductance in repeated junction-forming and -breaking cycles while simultaneously recording the conductance at a fixed bias of only 10 mV and at 300 K. In this low-bias regime, one probes the local density of states (LDOS) around the Fermi energy of the leads ( $E_{F,Au} = 5.1$ – $5.4$  eV), which is dominated by the two narrowest molecular orbitals. Individual conductance traces reveal distinct steps where the conductance varies only a little over some tenths of a nanometer (Figure 2A). These plateaus indicate that a small number (down to one) of molecules bridge the gap between the two electrodes. Control experiments in the absence of molecules, in which the distance-dependent electron tunneling current in vacuum was recorded, exhibit an exponential distribution of conductance values, as indicated by the gray dotted line in Figure 2B. The current traces (measured from  $1 G_0$  to  $10^{-8} G_0$ ) are 20–100 times shorter overall than the traces recorded in the presence of molecules. When the statistics of 500 such molecular opening traces are plotted in a conductance histogram, two distinct peaks with narrow distributions are revealed, with conductance values of  $1.7 \times 10^{-3} G_0$  and  $1.1 \times 10^{-3} G_0$  (Figure 2B). The averaged conductance ratio for the two distributions is 1.5. In the test experiments without

molecules, the distribution is exponential, as indicated by the gray dotted line in Figure 2B. It is important to mention that the data shown in Figure 2B represent raw data, and no filtering based, for example, on data selection rules was applied in order to unmask the molecular peaks.

As the junction is closed up to  $(15 \pm 5) \times G_0$  in every closing cycle, the molecular junction is broken and re-established in every cycle (roughly only every third cycle shows the signature for trapping molecules). As a consequence, the number of molecules and the microscopic details of the junction (different binding sites, different electric field gradients across the molecule, etc.), as well as the polarity of the molecules with respect to the applied bias, can change completely from cycle to cycle. Therefore, the experiment probes molecules in both forward and reverse polarization, as illustrated in the inset in Figure 2B. The two distinct distributions hence clearly indicate that the molecular junction has two different conductance values measured at a fixed voltage of 10 mV depending on how the molecule is oriented in the junction. Also noticeable is that the two situations occur with almost the same probability represented by the same peak height after subtraction of the electron co-tunneling background. Remarkably, these two conductance values of  $(1.1 - 1.7) \times 10^{-3} G_0$  are almost 10 times higher than the one measured in the self-assembled monolayer (SAM) architecture<sup>12</sup> with  $1.5 \times 10^{-4} G_0$ . In contrast to the a.c. method used to gently approach the SAM,<sup>12</sup> we go into direct metal–metal contact and close the junction in every cycle up to  $(15 \pm 5) \times G_0$ . Hence we establish a chemical bond to both electrodes instead of having only a tunneling contact to the STM tip, which easily reduces the measured conductance by 1 order of magnitude. Furthermore, the higher conductance of the single molecule measured here can also be explained by the more constrained situation of the ensembles of molecules in a SAM at ambient conditions. We speculate that while on the one hand intermolecular transport in the SAM opens additional transport channels across the SAM and hence increases the conductance, steric hindrance in the SAM can, on the other hand, drastically lower the conductance.

**Variable-Bias Current–Voltage Spectroscopy.** More insight into the nonlinear transport properties of molecular building blocks is provided by current–voltage,  $I$ – $V$ , characteristics when the bias window is sufficiently large to probe the first molecular levels in resonance.<sup>17</sup> In particular for rectification,  $I$ – $V$  characteristics at different temperatures can provide conclusive answers about the intrinsic functionality embodied in single molecules as well as about the underlying transport mechanisms. At 300 K, a voltage of  $\pm 1.5$  V can be applied to the Au–diode–Au junction in a nondestructive way, meaning that several  $I$ – $V$  curves

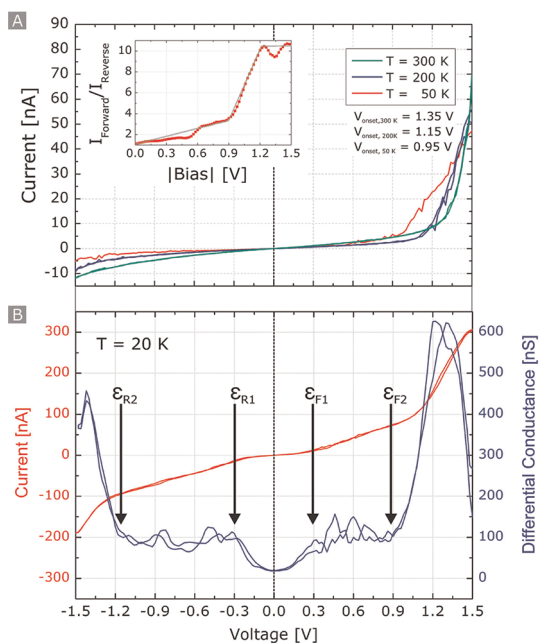


**Figure 3.** (A)  $I$ – $V$  traces for the Au–SB diode–Au junction recorded at temperatures ranging from 300 to 50 K. The inset shows the rectification ratio as a function of bias for 50 K (red dotted line as a guide to the eye). (B)  $I$ – $V$  and  $G_{\text{diff}}$ – $V$  curves for 20 K showing different molecular levels in resonance. The first resonant energy level is located at  $\pm 0.3$  V, the second level at  $+0.9$  V in forward bias, and at  $-1.2$  V in reverse bias.

can be acquired that carry reproducible features and similar current levels for a fixed electrode distance. In contrast to similar organic compounds measured so far,<sup>18</sup> the  $I$ – $V$  curves of the diode molecule exhibit certain characteristics distinctly different from the typical pure exponential tunneling curves over the entire temperature range probed, even at 300 K. For the forward direction with respect to reverse bias, a strong asymmetry in the junction current is observed (red curve in Figure 3). This pronounced asymmetry is very robust against small changes ( $<0.1$  nm) in the gap distance and thus cannot be attributed to possible asymmetries in the molecule–metal coupling alone. For example, different binding sites for the S–Au bond can lead to only weakly ( $<50\%$ ) asymmetric  $I$ – $V$  curves. Control measurements on quaterphenyl molecules revealed symmetric  $I$ – $V$  characteristics with slightly higher currents on both voltage branches (80–100 nA at  $\pm 1.5$  V). Remarkably, the diode molecule shows no degradation at 300 K (for an increasing number of cycles) as reported earlier in SAMs.<sup>19</sup> The “zero-bias conductance” at 300 K is around  $7.0 \times 10^{-4} G_0$  (linear interpolation of data points between  $\pm 25$  mV) and agrees well with the value of  $(1.1 - 1.7) \times 10^{-3} G_0$  determined by the low-bias histogram measured at the same temperature.

After having established a Au–diode–Au junction at room temperature, the system is cooled slowly ( $<5$  K/min) and the electrode position adjusted according

to the changed gap distance due to thermal shrinkage upon cooling using a feedback mechanism. This allows the temperature dependence to be studied on a single-molecule level as demonstrated here. Using the feedback mechanism, the Au–diode–Au junction can be cooled to 50 K without losing the molecule bridging the gap between the left and the right electrode. This process is assisted by the high flexibility of the thiol linker (most presumably attached to Au adatom or cluster) on the Au surface upon mechanical manipulation. The electrode withdrawing due to the shrinkage of the underlying polymer layer is substantial and corresponds to more than 2 nm distance change for  $\Delta T = 250$  K (measurement of the electron tunneling current for an open junction). The typical adjustment procedure is shown in the inset of Figure S1 in the Supporting Information.

All  $I$ – $V$  curves recorded, independent of the temperature, reveal a pronounced current rectification with the largest values as much as 11 ( $I_F(V = +1.5 \text{ V})/I_R(V = -1.5 \text{ V})$ ). The moderate current amplitude on the order of 45–70 nA at +1.5 V as well as the strong asymmetry indicates that transport occurs through an individual molecule rather than an ensemble of molecules. If more than one molecule were captured randomly, the probability to measure rectification would be half the one in the case of a single molecule since the two molecules can also be oriented opposite to each other. For a larger number of molecules, the orientation of them would average out asymmetric features such as rectification because the polarity of the molecules cannot be controlled in the experiment as mentioned earlier. The maximal current (at +1.5 V) changes only between 45 and 70 nA if the temperature is varied (the reverse current from 6 to 11 nA). The small differences are not consistent with a rectification mechanism based on thermally activated processes (e.g., thermally induced injection barrier lowering). The fact that we observe rectification at all temperatures indicates a mechanism that is largely independent of temperature. The magnitude of differences in the observed currents lie within the range of what is expected for small variations in contacting geometry on the atomic scale. Details of the functional  $I$ – $V$  behavior, however, may depend on the temperature. The current onset, for example, at forward bias, shifts from 1.35 V (300 K), 1.15 V (200 K), and 0.95 V (50 K) to 0.3 V (20 K) (see Figure 3A). For forward biases larger than 1.8 V, the molecular junction becomes unstable and fuses into a metal–metal contact, as already reported for the same molecule.<sup>12</sup>

Except for the strong asymmetry, the molecular fingerprint of the molecule given by resonant energy levels is rather weak compared with that of other molecules and is revealed only at very low temperatures. At 20 K, two resonant molecular orbitals are revealed, as shown in Figure 3B. Here, the rectification

is weaker and the ratio reaches only 1.5 at 1.5 V. The higher current level indicates that the biphenyl and the dipyrimidinyl rings now lie more in-plane because of reduced rotational vibrations, which leads to a larger overlap between the two subsystems and hence an increase in the current. Remarkably for the diode molecule, when compared with quaterphenyl (or any other similar molecule), the first resonant structures become only visible at 20 K, whereas for quaterphenyl, resonant peaks<sup>18</sup> appear already at 150 K and become much more pronounced at approximately 100 K. For the diode molecule, the conductance gap is found to be approximately 0.3 V with a zero-bias conductance around 18 nS, slightly lower than the value measured at 300 K (54 nS). At 0.3 V, the first molecular orbital is aligned with the chemical potential of one of the electrodes and opens a resonant tunneling path with largely increased transmission for holes (rather than electrons<sup>12</sup>). At higher voltages, the current amplitude remains almost constant until another molecular energy level gets energetically into resonance. This happens at +0.9 and –1.2 V (shown in Figure 3). These resonances are asymmetric in bias because of the presence of the donor and the acceptor moieties in the molecular backbone. Current flow in the forward direction starts when the donor moiety opens up a resonant path for electron transmission at +0.9 V, and current rectification is revealed when the acceptor moiety gets energetically into transmission at –1.2 V. For higher bias, no further molecular orbitals fall into the bias window<sup>5</sup> and the current saturates. The onset of transport in the forward direction at +0.9 V is also reflected in the rectification curves (inset in Figure 3A) recorded at higher temperatures. The onset agrees perfectly with calculated  $I$ – $V$  curves<sup>12,14</sup> and is explained by a strong asymmetrical localization of the hole ground-state wave function under the applied electrical field. Here the current rectification starts at approximately 0.9 V and saturates at 1.2 V. This can be explained by the second energy level of the molecule getting into resonance. The current values measured at voltages of 0.9 V are in very good agreement with previous measurements.<sup>12</sup>

**Diode Modeling.** To understand the underlying physical mechanisms governing the rectification behavior, we consider the two prominent mechanisms proposed in the literature. The first proposal by Aviram and Ratner<sup>1</sup> is depicted in Figure 4A. Here, the transport through a molecule involves three tunneling steps (represented by rates  $\Gamma_i$ ) from the electrodes through two separate energy levels,  $\varepsilon_1$  and  $\varepsilon_2$  (with respect to the Fermi energy of the electrodes,  $E_{F,Au}$ ). According to the proposal, these two levels belong to an electron donor and acceptor, respectively. The two levels respond differently to the electric field between the electrodes upon application of a bias voltage. As a consequence, the two levels may align or misalign

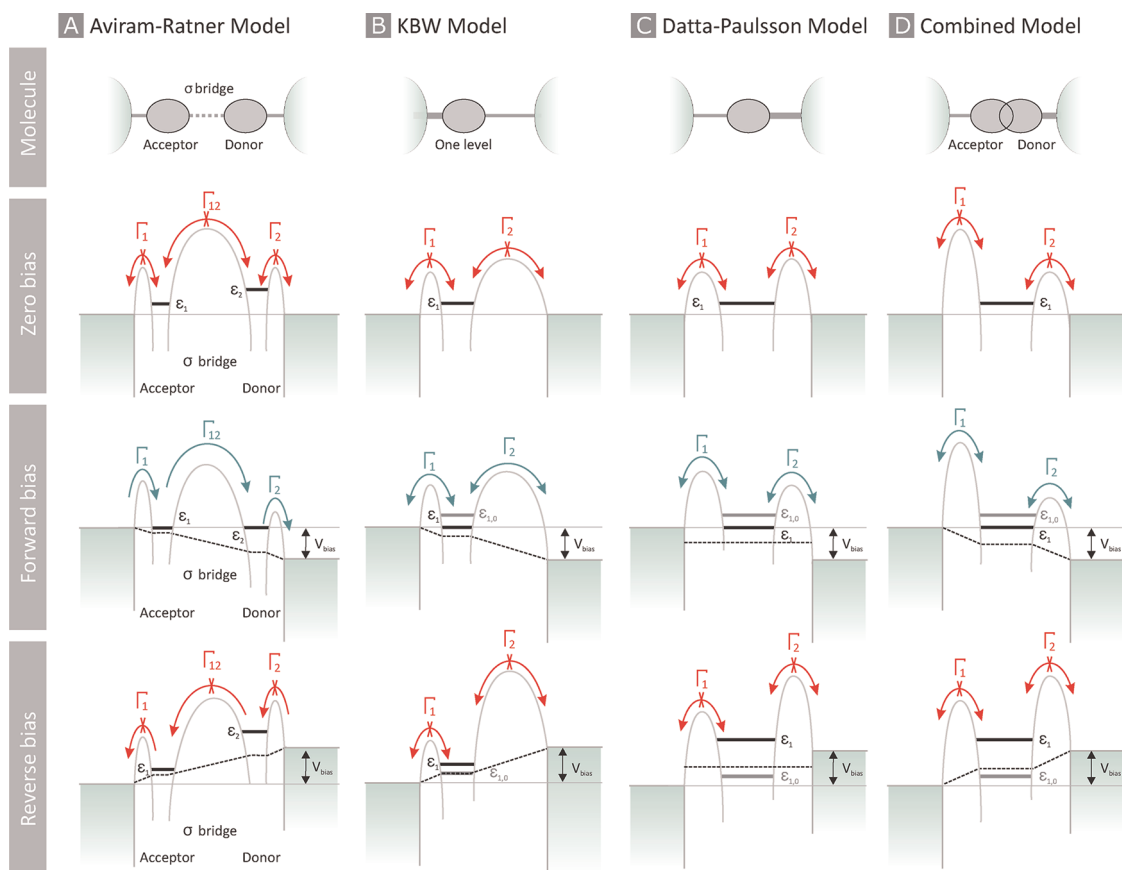


**Figure 4.** Comparison of models for molecular diodes. (A) Aviram–Ratner proposal with molecule levels shifting through the applied electric field. The different level spacings for donor and acceptor moieties, in combination with the large electrical spacer separating the two moieties, finally leads to a difference in the current onset. (B) Simplified model as proposed by Kornilovitch, Bratkovsky, and Williams (KBW) with one level. The level is shifted with respect to applied electric field. (C) Considering the charging of the energy levels (proposed by Datta and Paulsson) can also lead to diode behavior, even without level shifting by an electric field. (D) Combining the two models leads to a pronounced diode behavior, especially for asymmetric level couplings, as given by the asymmetric SB diode molecule. The potential (gray solid lines) and the electric field (black dotted lines) between the electrodes are plotted schematically. The discrete molecular energy levels (thick lines)  $\epsilon_1$  and  $\epsilon_2$  can be shifted due to electric field (A,B), through charging (from  $\epsilon_{1,0}$  to  $\epsilon_{1,r}$  and  $\epsilon_{2,0}$  to  $\epsilon_{2,r}$ ) (C), or through a combination thereof (D). In this schematic, only one energy level is used in model (D) for clarity reasons. The model fit described in the text uses two levels. These are, however, not in series as in (A), but in parallel; *i.e.*, they inhabit the same potential well (see Supporting Information).

depending on the sign of the applied voltage. The asymmetry in the charge transport of such an Aviram–Ratner diode is essentially seen as a different onset of resonant tunneling for the two bias directions. In our case, however, there is a small difference between  $\Gamma_{1,l}$  and  $\Gamma_{1,r}$  and between  $\Gamma_{2,l}$  and  $\Gamma_{2,r}$  respectively. These differences in the onset voltages are much smaller than expected for a typical Aviram–Ratner diode. In addition to the characteristic current onsets, also the current slopes carry information about the underlying transport mechanism.<sup>5</sup> The higher the charging energy of a molecular state, the smaller is the differential conductance. As argued below, this can lead to a completely different type of rectification in a molecular junction. Note also that although a donor and an acceptor part are incorporated into our molecule, these two moieties are not strictly electronically decoupled but can overlap. Hence, it is more reasonable to assume two tunneling steps rather than three.

This leaves us with the two other proposed mechanisms of rectification described above, namely, asymmetric level shifting by electric field and asymmetric level shifting through the charging energy. These two mechanisms are depicted in Figure 4B,C. We stress that although these two mechanisms are not easily separated in the practical implementation, they show the necessary ingredients for a full description of the rectification process. The two mechanisms have different influence on the resulting current–voltage characteristics: the asymmetric field mechanism leads to a shift in onset voltage for resonant tunneling depending on bias direction. The asymmetric charging leads to a different differential conductance in the region of resonant tunneling.<sup>6</sup> In either case, these diode types require a different coupling of the relevant orbital to the two electrodes. The asymmetric field argument (Figure 4B) is rather obvious from the asymmetric design of the molecule in the first place. The

asymmetric tunneling barrier (Figure 4B), however, is also plausible for our experiment. In general, asymmetric tunneling barriers between the orbital and the metal electrodes can be induced first, by the type and the strength of the chemical bond established between the anchoring moiety and the electrode and, second, by the bonding site of the anchor group on the electrode surface. The latter effect depends on the specific microscopic configuration of the molecule–metal interfaces and can lead to small rectification effects (<50%) even in symmetric molecules. As discussed above, asymmetries in the two bonding sites can be minimized by careful jiggling of the electrode distance. In contrast, the molecule used in this study can result in an asymmetric coupling to the electrodes because its aryl ring contains nitrogen only near one end of the molecule.

From this discussion, it becomes clear that neither of the three models (Aviram–Ratner, asymmetric field, asymmetric charging) can explain our data satisfactorily. Rather, we require a model that contains both asymmetric field and asymmetric charging. From the molecular structure, it is plausible that a combination of these two mechanisms is the origin for the observed rectification effect. To understand the underlying transport mechanisms and to extract all of the physical parameters, such as energy-level position, energy-level coupling, and field gradient across the junction, we propose a simple two-level model consisting of a diblock molecule, as illustrated in Figure 1A. This approach uses the semiempirical formalism (a “toy model”) proposed by Datta and Paulsson *et al.*<sup>5</sup> To combine the mechanisms of level shifting by field (Figure 4A,B) and by the charging (Figure 4C), we derived the model depicted in Figure 4D. The resonant tunneling through two levels *in series* of the Aviram–Ratner (AR) model is replaced by a single level, as argued above. However, of such unified extended electronic states, we will need two, acting *in parallel* (instead of AR’s levels in series) to account for the different current onsets observed in experiment. Here, each of the molecular levels (for clarity, only one of the levels is shown in Figure 4D) is characterized by an energy level, a charging energy, two (different) rates of coupling to the two electrodes, and a parameter describing a shift of energy in response to application of a bias.

**Fitting Results.** To account for the two molecular levels, we fit the data using a superposition of two single orbital models (Figure 4C) (see Supporting Information for a full description), one for a closer and one for a higher energy level with respect to  $E_{F,Au}$ . The resulting two current paths are coupled by their charging energies. In our implementation, the charging of either level produces an equivalent shift of the other level. The latter assumption was made because the experimental data do not contain sufficient

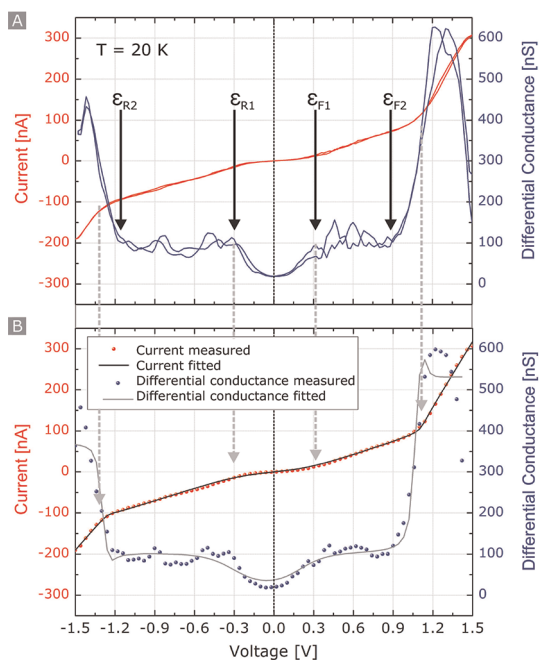


**Figure 5.** (A)  $I$ – $V$  curves taken at 20 K revealing four resonant energy levels. (B) Fitting of the  $I$ – $V$  curves to a single-level semiempirical model. The black curve shows the calculated current values, the gray curve the first derivative. The gray arrows indicate the resonant peaks, which are in good agreement with the fitted curve.

information to distinguish this from more complex cases (*i.e.*, two instead of the four charging energy values proposed by Datta and Paulsson were used). As a result, a least-squares fit of the data as shown in Figure 5 yielded  $\epsilon_1 = 0.099$  eV and  $\epsilon_2 = 0.48$  eV, as is already apparent from the raw data. Furthermore,  $\epsilon_1$  is coupled to the left and the right electrode with  $\Gamma_{1,l} = 3.2 \times 10^{-3}$  eV and  $\Gamma_{1,r} = 3.5 \times 10^{-3}$  eV, respectively. The respective rates of  $\epsilon_2$  are  $\Gamma_{2,l} = 4.2 \times 10^{-3}$  eV and  $\Gamma_{2,r} = 3.2 \times 10^{-3}$  eV, reflecting the asymmetry of the  $I$ – $V$  curves. The absolute values are fitting parameters to obtain the correct magnitude of the current. Most interesting, however, is the asymmetry of the  $I$ – $V$  curves given by the ratio of the rates. These ratios are 0.9 and 1.3 for levels 1 and 2, respectively. Finally, the charging energies are 3.9 and 0.98 eV, respectively. The charging energy describes the shift of the corresponding electronic energy level per unit charge dwelling on the molecule.<sup>6</sup> The second fitting value of 0.98 eV is typical for single molecules, the first value seems to be quite large, and the ratio between the rates is consistent with the experimental observation. The fit parameters of the first energy level, however, are less useful. We note that the fit parameters are influenced by fitting the measurement data in the conductance gap (see Figure 3B). The underlying issue is that the model does not take into account any nonresonant transport around zero bias except through broadening of the state 1. For example, direct electrode–electrode tunneling bypassing the molecule may have some very

small but significant effect. This leads to an artificially high charging energy and a larger uncertainty in the ratio of rates. Nevertheless, the main source of rectification is clearly the resonant transport through the second level and can be explained well using our model. Figure 5 shows the derived fit of the experimental data taken at 20 K (Figure 3).

## SUMMARY

In summary, we have demonstrated that unimolecular current rectification occurs in a donor–acceptor-type diblock dipyrimidinyl diphenyl molecule both in the low-bias and the variable voltage regime. The distinct peaks in the histograms demonstrate

that the molecule is trapped in the two polarizations with equal probability. The rectification in the  $I$ – $V$  curves were found to be independent of temperature in the range of 300 to 50 K. The rectification ratio of up to 11 is among the highest values reported for single molecules. Asymmetric resonant hole transport was simulated by a novel diode model which yielded excellent agreement to experimental data. The simple concept of diblock molecules containing electronic functionality opens up the exciting possibility to use these molecular diodes in single-molecule cross-bar structures, such as a unimolecular extension of a switching or charge-storing building block.

## EXPERIMENTAL SECTION

**Mechanically Controllable Break-Junction Technique.** For all transport measurements including low-bias conductance histograms and variable-bias current–voltage experiments, we used the mechanically controllable break-junction (MCBJ) technique. The system is mounted on a helium cryostat (with a temperature range from 4 to 350 K) in an ultrahigh vacuum (UHV) chamber. All measurements are conducted at a pressure of  $2 \times 10^{-9}$  mbar.

**Chip Fabrication.** Electron-beam lithography (JEOL JSM-6301F, 100 keV) in combination with a lift-off technique (PMMA 950 K 4% Anisol lifted by Aceton) and isotropic reactive ion etching ( $O_2$  50 sccm flow, 200 W, 7 min) is employed to structure a freestanding gold bridge on a flexible, insulating substrate (250  $\mu$ m BeCu, 6  $\mu$ m polyimide; see Figure 1A). After the initial breaking of the Au bridge by bending the metal substrate, a conditioning procedure is performed to shape the electrode tips until multiple integer values of the conductance quantum  $G_0 = 1/12.9$  k $\Omega$  (where  $G_0 = 2e^2/h = 77.4$   $\mu$ S,  $e$  the electron charge, and  $h$  the Planck constant) are observed, indicating the formation of atomically sharp electrode tips.

**Deposition of Molecules.** The diode molecules were dissolved in very low concentration in tetrahydrofuran (THF) ( $4 \times 10^{-5}$  mol/L). In the MCBJ geometry, both electrodes consist of the same material, hence the possibility of an oriented alignment *via* sequential deprotection (see main text) of the terminal groups is not applicable. As a consequence, deprotection was carried out simultaneously on both ends of the molecule in one step, using a solution of tetrabutylammonium fluoride (TBAF) in THF. During 5 min, the molecules deposited from solution can absorb onto the open junction's surface. During the deposition time, the system is purged with nitrogen. Without subsequent rinsing, the system is then evacuated again.

**Electrical Measurements.** All measurements were performed using an Agilent 4156B semiconductor parameter analyzer with high-resolution source-measure units (1 fA resolution). We are using a statistical measurement approach,<sup>17</sup> which facilitates the investigation of the transport properties of a single-molecule junction during its formation and breaking. For each run in both low-bias conductance as well as variable-bias current–voltage spectroscopy experiments, the junction is closed up to  $25 G_0$  in order to ensure a completely new configuration of the junction for the next measurement cycle.

**Conflict of Interest:** The authors declare no competing financial interest.

**Acknowledgment.** We are grateful to W. Riess, C. Schönenberger, and J. M. van Ruitenbeek for scientific discussions. This research was supported financially by the European Community (FP7/2007-2013) under the grant agreement “SINGLE” no. 213609. L.Y.'s group acknowledges partial support from NSF and NSF-MRSEC project at the University of Chicago.

*Supporting Information Available:* Additional experimental data as well as an extended description of the model is available. This material is available free of charge *via* the Internet at <http://pubs.acs.org>.

## REFERENCES AND NOTES

- Ratner, M. A.; Aviram, A. Molecular Rectifiers. *Chem. Phys. Lett.* **1974**, *29*, 277–283.
- Ratner, M. A. Introducing to Molecular Electronics. *Mater. Today* **2002**, *5*, 20–27.
- Ellenbogen, J. C.; Love, J. C. Architectures for Molecular Electronic Computers: 1. Logic Structures and an Adder Designed from Molecular Electronic Diodes. *Proc. IEEE* **2000**, *88*, 386–426.
- Kornilovitch, P. E.; Bratkovsky, A. M.; Williams, R. S. Current Rectification by Molecules with Asymmetric Tunneling Barriers. *Phys. Rev. B* **2002**, *66*, 165436.
- Datta, S.; Tian, W.; Hong, S.; Reifenberger, R.; Henderson, J. I.; Kubiak, C. P. Current–Voltage Characteristics of Self-Assembled Monolayers by Scanning Tunneling Microscopy. *Phys. Rev. Lett.* **1997**, *79*, 2530–2533.
- Paulsson, M.; Zahid, F.; Datta, S. In *Handbook of Nanoscience, Engineering, and Technology*; Goddard, W., III, Brenner, D. W., Lyshevski, S. E., Iafate, G. J., Eds.; CRC Press: Boca Raton, FL, 2003.
- Metzger, R. M.; Chen, B.; Höpfner, U.; Lakshminathan, M. V.; Vuillaume, D.; Kawai, T.; Wu, X.; Tachibana, H.; Hughes, T. V.; Sakurai, H.; *et al.* Unimolecular Electrical Rectification in Hexadecylquinolinium Tricyanoquinodimethanide. *J. Am. Chem. Soc.* **1997**, *119*, 10455–10466.
- Metzger, R. M. Unimolecular Electrical Rectifiers. *Chem. Rev.* **2003**, *103*, 3803–3834.
- Ng, M. K.; Lee, D.-C.; Yu, L. Molecular Diodes Based on Conjugated Diblock Co-oligomers. *J. Am. Chem. Soc.* **2002**, *124*, 11862–11863.
- Jiang, P.; Morales, G. M.; You, W.; Yu, L. Synthesis of Diode Molecules and Their Sequential Assembly To Control Electron Transport. *Angew. Chem., Int. Ed.* **2004**, *116*, 4571–4575.
- Elbing, M.; Ochs, R.; Koentopp, M.; Fischer, M.; von Hänisch, C.; Weigend, F.; Evers, F.; Weber, H. B.; Mayor, M. Single-Molecule Diode. *Proc. Natl. Acad. Sci. U.S.A.* **2005**, *102*, 8815–8820.
- Diez-Perez, I.; Hihath, J.; Lee, Y.; Yu, L.; Adamska, L.; Kozhushner, M. A.; Oleynik, I. I.; Tao, N. Rectification and Stability of a Single Molecular Diode with Controlled Orientation. *Nat. Chem.* **2009**, *1*, 635–641.
- Cuevas, J. C.; Scheer, E. *Molecular Electronics: An Introduction to Theory and Experiment*; World Scientific: River Edge, NJ, 2010.



14. Morales, G. M.; Jiang, P.; Yuan, S.; Lee, Y.; Sanchez, A.; You, W.; Yu, L. Inversion of the Rectifying Effect in Diblock Molecular Diodes by Protonation. *J. Am. Chem. Soc.* **2005**, *127*, 10456–10457.
15. Muller, C. J.; van Ruitenbeek, J. M.; de Jongh, L. J. Experimental Observation of the Transition from Weak Link to Tunnel Junction. *Physica C* **1992**, *191*, 485–504.
16. Moreland, J.; Elkin, J. W. Electron Tunneling Experiments Using Nb-Sn “Break” Junctions. *J. Appl. Phys.* **1985**, *58*, 3888–3895.
17. Lörtscher, E.; Weber, H. B.; Riel, H. Statistical Approach To Investigating Transport through Single Molecules. *Phys. Rev. Lett.* **2007**, *98*, 176807.
18. Lörtscher, E.; Elbing, M.; Tschudy, M.; von Hänisch, C.; Weber, H. B.; Mayor, M.; Riel, H. Charge Transport through Molecular Rods with Reduced  $\pi$ -Conjugation. *Chem. Phys. Chem.* **2008**, *9*, 2252–2258.
19. Metzger, R. M.; Panetta, C. A. *J. Chim. Phys.* **1988**, *85*, 1125–1134.